HAZARDS FROM UNDERWATER EXPLOSIONS

by

Michael M. Swisdak, Jr.
and
Paul E. Montanaro

ABSTRACT

The airblast and fragmentation produced in air by underwater explosions has been reexamined and reanalyzed. The data were examined with the following questions in mind: (1) At what range does the Inhabited Building Distance (1.2 psi) and the Public Withdrawal Distance (0.07 psi) occur? (2) What are the fragmentation characteristics (velocity, launch angle, dispersion, mass) produced by underwater explosions? Both goals were met. A series of equations relating overpressure to scaled depth and scaled distance are derived and presented. Similarly, equations relating fragmentation characteristics to scaled depth are derived.

INTRODUCTION

Recently, there has been an increased interest in using both water-filled quarries and man-made ponds for underwater explosion testing. This has led to questions which must be answered for any new facility: (1) What is the Inhabited Building Distance? (2) What is the Public Withdrawal Distance? and (3) What are the fragmentation characteristics produced by the tests?

To answer these questions, the Department of Defense Explosives Safety Board asked the Naval Surface Warfare Center to review the available data and then to propose empirically-based prediction methodologies. This paper describes the result of that effort.

AIRBLAST

The airblast produced by underwater explosions is a complicated phenomenon. In general a multi-pulse wave train is produced. Depending upon the scaled depth of burst (depth divided by the cube root of an effective charge weight), the scaled range (range divided by the cube root of an effective charge weight), and the type of explosive either the first, second, and sometimes later pulses may have the largest amplitude. At some depths the maximum pulse is produced by the underwater

Report Documentation Page

Form Approved
OMB No. 0704-0188

1. REPORT DATE **AUG 1992**	2. REPORT TYPE	3. DATES COVERED **00-00-1992 to 00-00-1992**
4. TITLE AND SUBTITLE **Hazards from Underwater Explosions**		5a. CONTRACT NUMBER
		5b. GRANT NUMBER
		5c. PROGRAM ELEMENT NUMBER
6. AUTHOR(S)		5d. PROJECT NUMBER
		5e. TASK NUMBER
		5f. WORK UNIT NUMBER
7. PERFORMING ORGANIZATION NAME(S) AND ADDRESS(ES) **Naval Surface Warfare Center,Indian Head Division,10901 New Hampshire Avenue,Silver Spring,MD,20903-5640**		8. PERFORMING ORGANIZATION REPORT NUMBER
9. SPONSORING/MONITORING AGENCY NAME(S) AND ADDRESS(ES)		10. SPONSOR/MONITOR’S ACRONYM(S)
		11. SPONSOR/MONITOR’S REPORT NUMBER(S)

12. DISTRIBUTION/AVAILABILITY STATEMENT
Approved for public release; distribution unlimited

13. SUPPLEMENTARY NOTES
See also ADA261116, Volume IV. Minutes of the Twenty-Fifth Explosives Safety Seminar Held in Anaheim, CA on 18-20 August 1992.

14. ABSTRACT
see report

15. SUBJECT TERMS

16. SECURITY CLASSIFICATION OF:			17. LIMITATION OF ABSTRACT	18. NUMBER OF PAGES	19a. NAME OF RESPONSIBLE PERSON
a. REPORT **unclassified**	b. ABSTRACT **unclassified**	c. THIS PAGE **unclassified**	**Same as Report (SAR)**	**18**	

explosion shockwave. At other depths, the maximum-amplitude pulse is produced by the oscillating explosion-products bubble. In a rigorous treatment, the amplitude and location of the pulses is also determined by the height above the surface at which the measurement is taken; i.e, at the same scaled range, gauges at two different heights may experience significantly different pulse forms.

For the purposes of this study, the only parameter of interest is the maximum pressure as a function of scaled depth and range. The range is the slant range between the point on the water surface above the detonation and the measurement point. Figure 1 is a sketch defining these parameters.

The original data were collected over a span of about 15 years by several agencies; most of the data, however, was collected by the Naval Ordnance Laboratory (now part of the Naval Surface Warfare Center). The data were collected in the following manner: An explosive charge of known weight and composition was detonated at a given depth. Airblast was measured at various heights and ranges above the water surface. Figure 2 is a sample for one depth of burst. As was indicated above, only the maximum pressure as a function of range is of interest. Figure 3 shows this sub-set of the Figure 2 data. For each scaled charge depth, a separate graph of maximum pressure versus scaled range was generated. For each such graph, a power law of the form:

$$P = A * Z^b \tag{1}$$

was fitted to the data using the method of least squares.

Here

P = maximum pressure (psi)
Z = scaled range ($ft/lb^{1/3}$) (range divided by the cube root of an effective charge weight)
A, b = fitting constants (A=Coefficient, b=Slope)

A sample of this type of curve fit is also shown in Figure 3. The results of these curve fits (values of A, b) and a measure of the goodness of fit generated by the least squares fitting process are shown in Table 1.

An examination of the value for the slope of the fit ("b" in the equation shown above) indicates that it approaches a value of 1 as the scaled depth of burst increases. This indicates that as the explosion source is moved deeper, the airblast decay approaches that of an acoustic wave with an amplitude proportional to 1/Z.

In the original data, the low pressure measurements were made at extremely long ranges (on the order of miles) because of the charge weights involved.

Propagation over long ranges always introduces weather-induced variations. To provide additional data in this regime which would not be as greatly affected by weather, a series of measurements was undertaken on a recent underwater test series. Here, the charge weights, depths, and ranges were such that the pressure levels of interest occurred at ranges of under 500 feet. Propagation over these shorter distances minimizes the effects of weather. In these tests, the scaled depth was greater than 10 ft/lb$^{1/3}$. Based on the information in Table 1, at this depth, the wave should exhibit acoustic decay (1/Z). This was assumed in the analysis. The raw data are presented in Table 2. The average coefficients determined from these data were added to those given in Table 1. This complete data set is presented in Table 3 and forms the basis for the development of the prediction equations. Table 3 is based upon data taken from several different types of explosives. These differences must be taken into account in any analysis. Table 4 presents a Weight Factor for each explosive. This Weight Factor is related to the underwater explosion bubble energy. When the actual explosive weight is multiplied by this Weight Factor, an effective charge weight is produced. This effective charge weight is then used in all subsequent calculations.

An examination of Table 3 indicates that both the Coefficient and Slope vary with scaled charge depth. Curve fits were made to both parameters as a function of scaled charge depth. These are shown in Figures 4 and 5. These curve fits were then used to generate Table 5. Either Table 5 or the curve fits shown in Figures 4 and 5 can be used to generate the airblast as function of depth and range.

For each scaled depth of interest, determine (from Table 5 or Figures 4 and 5) a coefficient and slope. These are then used in an equation of the form:

$$\mathbf{P = Coefficient * Scaled\ Range^{(slope)}}, \qquad (2)$$

where P is maximum pressure in psi and scaled range is in ft/lb$^{1/3}$.

These equations are valid over the following range:

$0.3 \text{ ft/lb}^{1/3} \leq \text{scaled depth} \leq 20 \text{ ft/lb}^{1/3}$

$4.0 \text{ ft/lb}^{1/3} \leq \text{scaled range} \leq 100 \text{ ft/lb}^{1/3}$.

As an example, determine the airblast at a range of 200 feet from the detonation of 1000 pounds of HBX-1 at a depth of 10 feet. For this same depth of burst and charge weight, determine the inhabited building range (1.2 psi) and the public withdrawal distance (0.07 psi). From Table 4, the Weight Factor is 1, so the effective weight is 1000 pounds. The scaled depth is 1.0 ($10/(1000)^{1/3}$) ft/lb$^{1/3}$ and the scaled range is 20 ($200/(1000)^{1/3}$) ft/lb$^{1/3}$. Entering Table 5, we find that the coefficient and slope are 11.63 and -1.02. Thus our prediction equation becomes:

$$P = 11.63 * Z^{-1.01}.$$

At a scaled range (Z) of 20 ft/lb$^{1/3}$, the predicted maximum pressure is 0.56 psi. This same prediction equation can be used to determine the ranges to 1.2 and 0.07 psi. The Inhabited Building Distance (range to 1.2 psi) would occur at a scaled range (Z) of 9.48 ft/lb$^{1/3}$; this corresponds to an actual range of 94.8 feet. The Public Withdrawal Distance (range to 0.07 psi) occurs at a scaled range of 157.9 ft/lb$^{1/3}$, corresponding to an actual range of 1579 feet. It must be pointed out however, that this prediction for public withdrawal distance is outside the validity range of the prediction equations and, therefore, must be used cautiously. It should be further noted that the prediction equation is designed to give the maximum pressure. Actual measurements at the specified location may be lower.

FRAGMENTATION

Previously, the throw of case fragments into the air from underwater detonations has, generally, been ignored. Statements such as "fragmentation was not considered" or "our experience is that we don't have a problem" have often been the rule.

Although considerable effort has gone into the study of fragmentation by weapons designed to explode in the air or the ground, very little information is available concerning fragmentation produced by underwater detonations. The only available data were generated during the investigation of the fragmentation produced by shallow explosions of MK 82 general purpose bombs. This extremely limited data set forms the basis for the prediction equations developed below.

In general, as the explosion source is moved deeper, the fragmentation problems are lessened--the launch velocities decrease (the fragments must travel through more water) and the fragment ejection angle becomes smaller. In order to describe the fragmentation, the following information is needed: vertical fragment velocity as a function of scaled depth of burst, the variation of the fragment velocity with launch azimuth, the maximum launch azimuth as a function of scaled depth of burst, and a description of the fragments (shape and mass). Descriptors for each of these will be developed in the following paragraphs. Figure 6 is a sketch defining the variables involved. It is based on the MK 82 tests from which most of the data are derived.

Figure 7 presents the variation in the vertical fragment velocity with scaled depth of burst. The two end points were not part of the original data set. At a zero depth of burst, the charge is half in the air and half in the water. Thus, the fragment velocity is simply the measured fragmentation velocity in air--approximately 8200 ft/s for a MK 82 bomb. The point at a scaled depth of 4 corresponds to evidence that for

scaled depths greater than about 4 $ft/lb^{1/3}$, there is no appreciable fragmentation. Also shown on the figure is a least squares curve fit to the data; this will be used for prediction purposes.

Figure 8 gives the variation of the fragment velocity as a function of launch azimuth. The data have been normalized to 1 for an azimuth of 0° (N.B.: 0° azimuth is vertical). As the scaled depth increases, the maximum azimuth angle decreases. This variation is shown in Figure 9. The two end points have been added to the data set. At the surface (scaled depth of zero), the fragments can come out in all 90° of azimuth. At a scaled depth of 4, other data indicate that, very few fragments escape. At the intermediate azimuths, Figure 9 gives the maximum azimuth at which the fragments can escape the water.

It must be pointed out, however, that the prediction equations generated in Figures 7-9 are for MK 82 bombs loaded with H-6 explosive. When the explosive is changed, the maximum velocity will also change. A velocity factor, derived from the Gurney Constant for each explosive composition is given in Table 4.

The fragments produced by underwater detonations are much larger than those produced by corresponding detonations on the surface. In the MK 82 underwater detonations, the fragments were long "spear-like" fragments rather than the usual chunky fragments. The worst-case fragments had length-to-width ratios of approximately 14, with a length approximately equal to the length of the cylindrical section of the bomb. Analysis indicated that these fragments, although spear-like, were best described with a Fragment Shape Factor of 0.25, indicating that, while spear-like, they are also tumbling.

There is now sufficient information to predict the fragmentation. For a given type explosive weight and charge depth, calculate the scaled depth of burst (actual depth of burst (measured to the center of gravity of the charge) divided by the cube root of the explosive weight). Using Figure 7, calculate the vertical fragment velocity. Next multiply this velocity by the velocity factor chosen from Table 4. This new velocity and Figure 8 gives the azimuthal velocity variation. Figure 9 is then used to determine the maximum azimuth angle. Determine the length of an equivalent cylindrical section of the explosive charge. A worst-case fragment has a length-to-width ratio of 14, so a width can be calculated. The fragment thickness should be taken as the thickness of the case. Knowing the case material, the weight of the fragment can then be calculated. The weight, velocities, and azimuths are then used as inputs to a trajectory program such as TRAJ[1], to predict maximum fragment range.

Let us consider two examples. During the MK 82 bomb underwater tests (described above), the locations of fragments recovered outside the water were mapped. One such fragment, weighing 800 grams, was found at a range of 1952 feet. This was the maximum range of all the fragments recovered on that test. The

explosive weight was 192 pounds of H-6; the center of gravity of the weapon was 2.25 feet below the water surface. This depth corresponds to a scaled depth of 0.39 ft/lb$^{1/3}$ (2.25/(192)$^{1/3}$). Using Figures 7-9, Table 6 can be generated as input for a trajectory program (TRAJ). The case material is steel and the fragment weight is 800 grams. The fragment shape factor is 0.25. The ranges determined by the trajectory program are also shown in Table 6. The maximum range is 1956 feet--matching almost exactly the measured range.

As a second example, let us consider the worst-case fragments produced by the detonation of a 1-to-1 cylinder of HBX-1 with an explosive weight of 10,000 pounds. The case thickness is 0.375" and the case material is steel. The depth of burst is 16 feet (measured to the center of the charge). A 1-to-1 cylinder containing 10,000 pounds of HBX-1 has a diameter of approximately 4.9 feet and a height of 4.9 feet. The scaled depth of burst is 16/(10,000)$^{1/3}$ or 0.74 ft/lb$^{1/3}$. Since the charge is cylindrical, the length of the cylindrical section is simply the height--4.9 feet. If we assume that a worst-case fragment has a length-to width ratio of 14, then the width is 4.9/14 or 0.35 feet. The fragment thickness is the case thickness, 0.375 inches. Thus the fragment weighs 26 pounds. The input conditions derived from Figures 7-9 and Table 4 are shown in Table 7. Also shown on this table are the results of the trajectory calculations. The maximum fragment range is 2888 feet.

It must be remembered that the ranges determined using this method are the maximum ranges--not the ranges at which the hazardous fragment density reaches a value of 1 per 600 ft^2.

REFERENCES

1. Montanaro, P. E., "TRAJ--A Two Dimensional Trajectory Program For Personal Computers," <u>Minutes of the Twenty-Fourth DoD Explosives Safety Seminar</u>, August 1990.

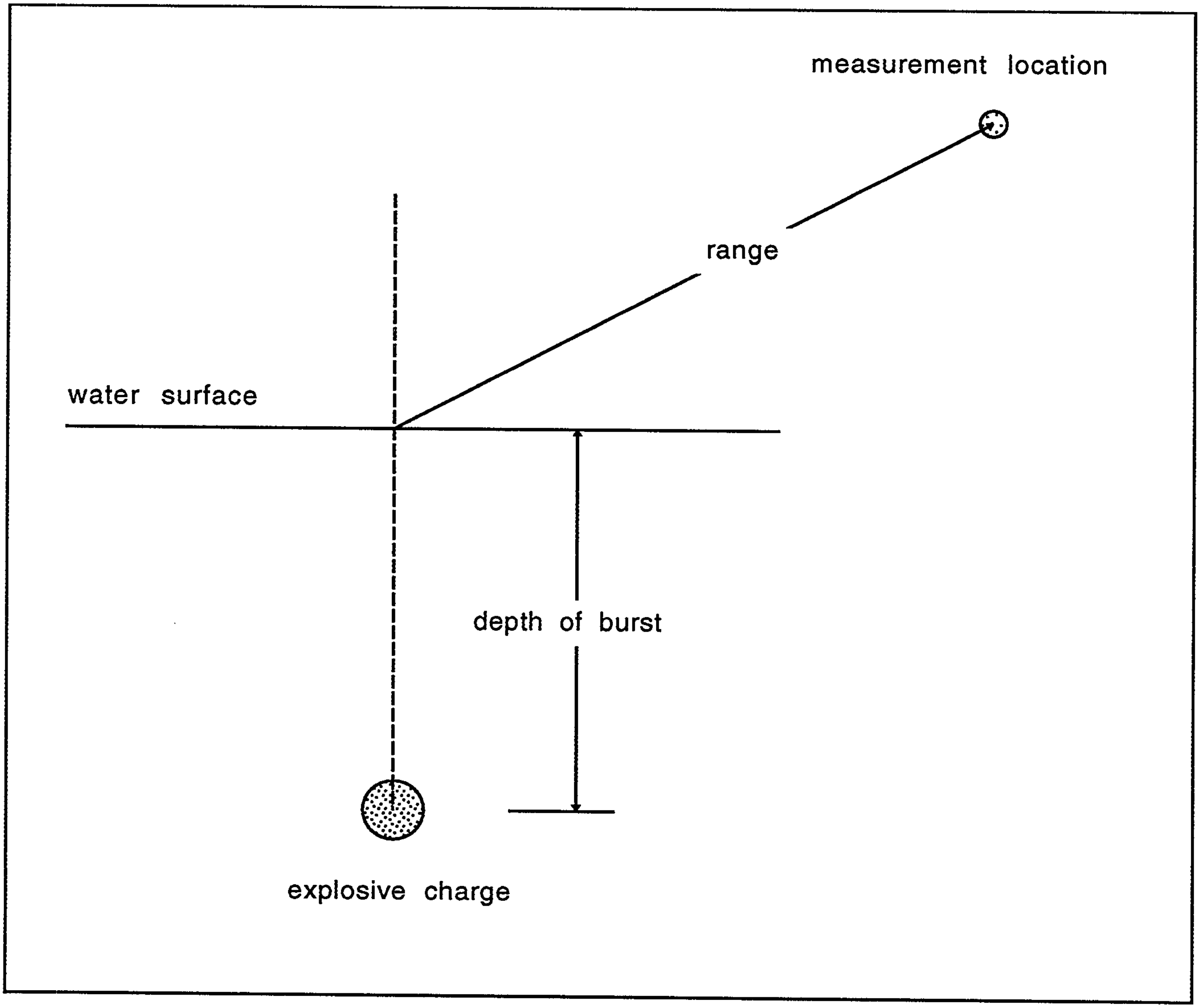

FIGURE 1 SCHEMATIC OF TEST ARRANGEMENTS

FIGURE 2. PRESSURE VERSUS SCALED RANGE

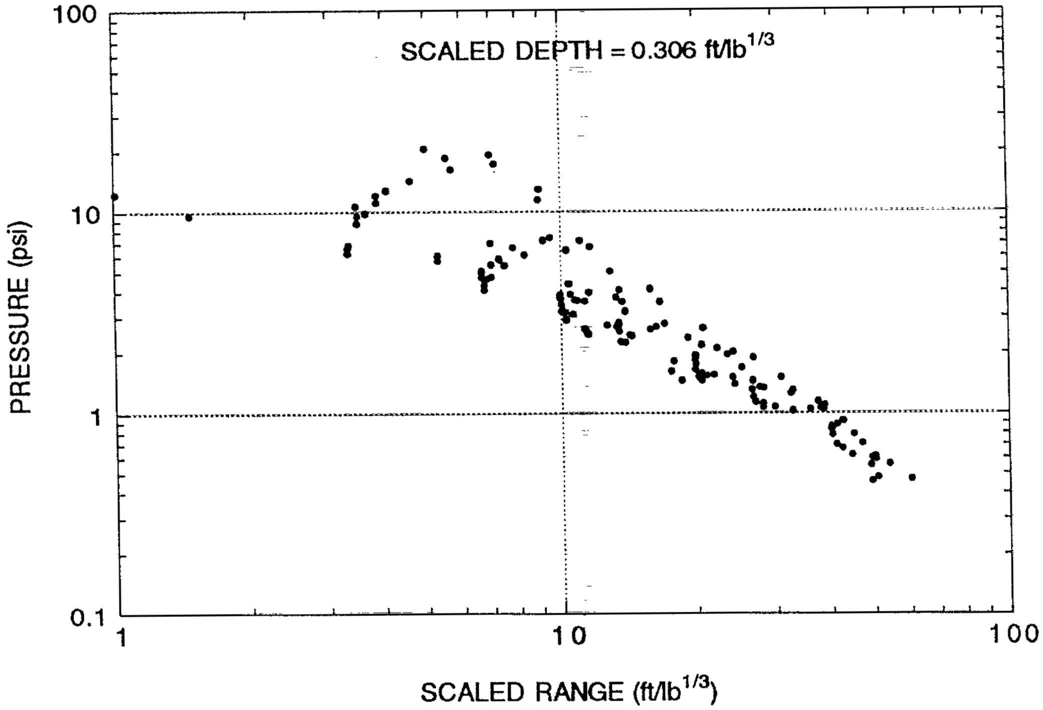

FIGURE 3. MAXIMUM PRESSURE VERSUS SCALED RANGE

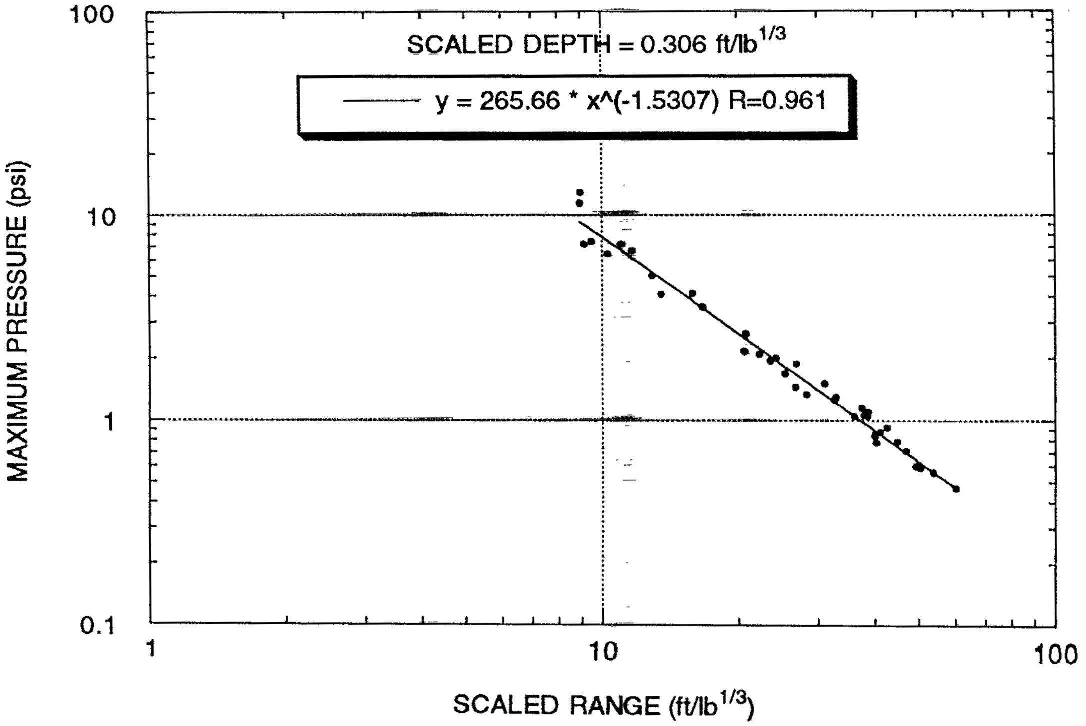

FIGURE 4. SLOPE VERSUS SCALED DEPTH OF BURST

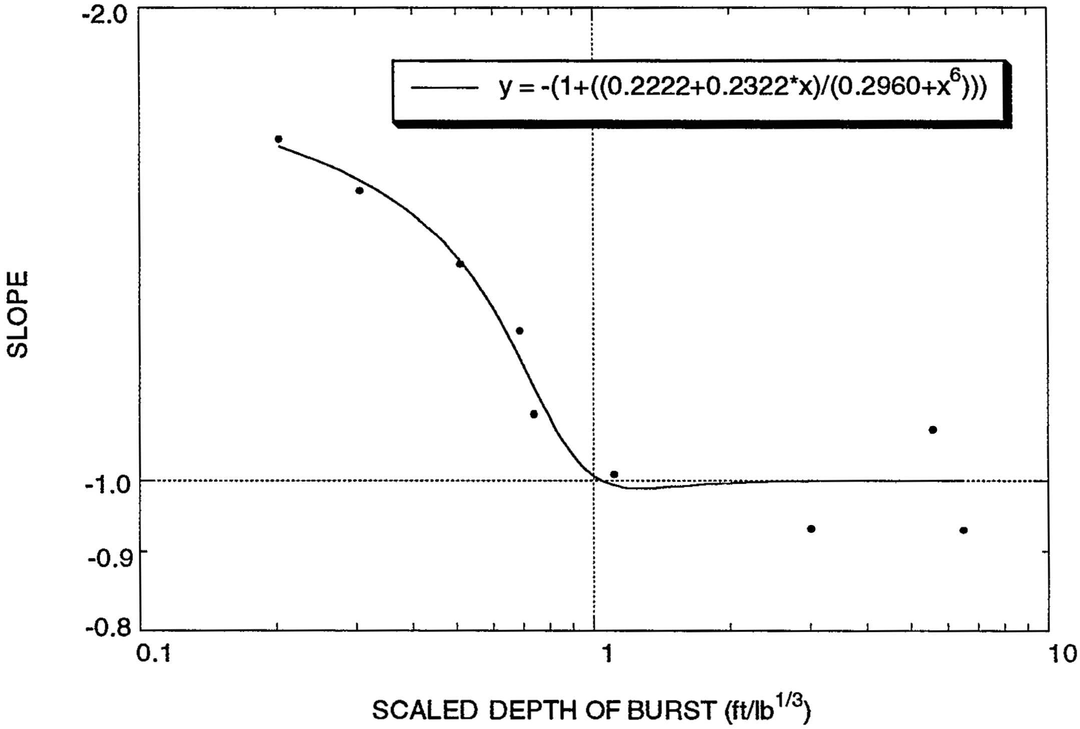

FIGURE 5. COEFFICIENT VERSUS SCALED DEPTH

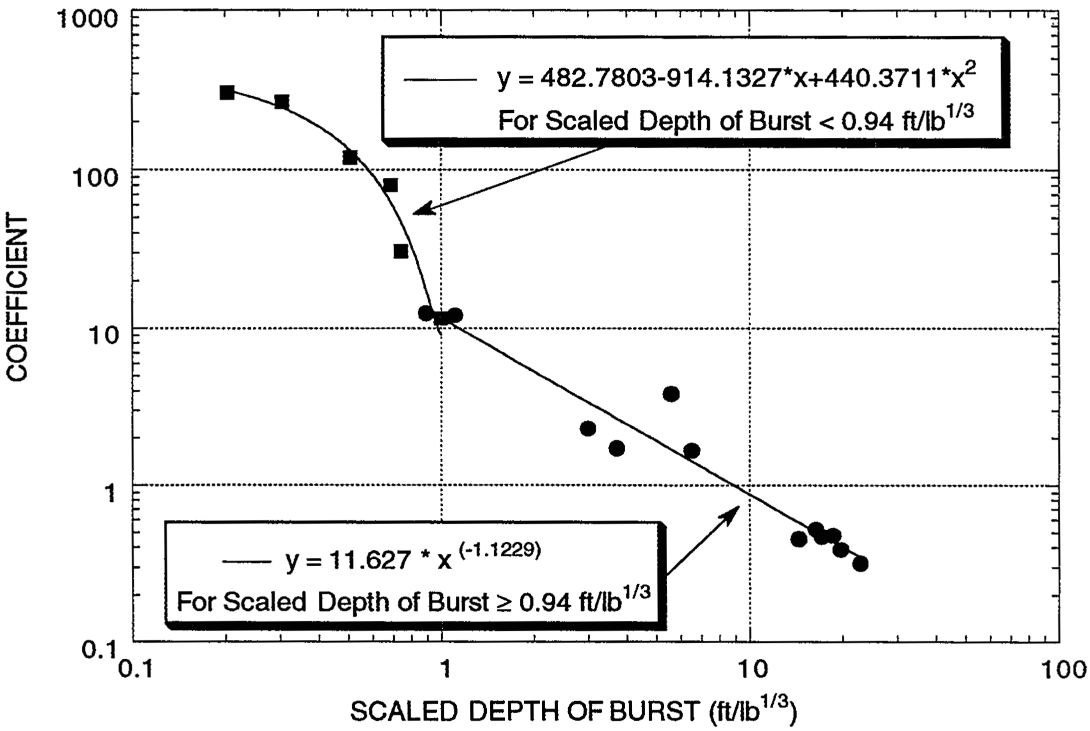

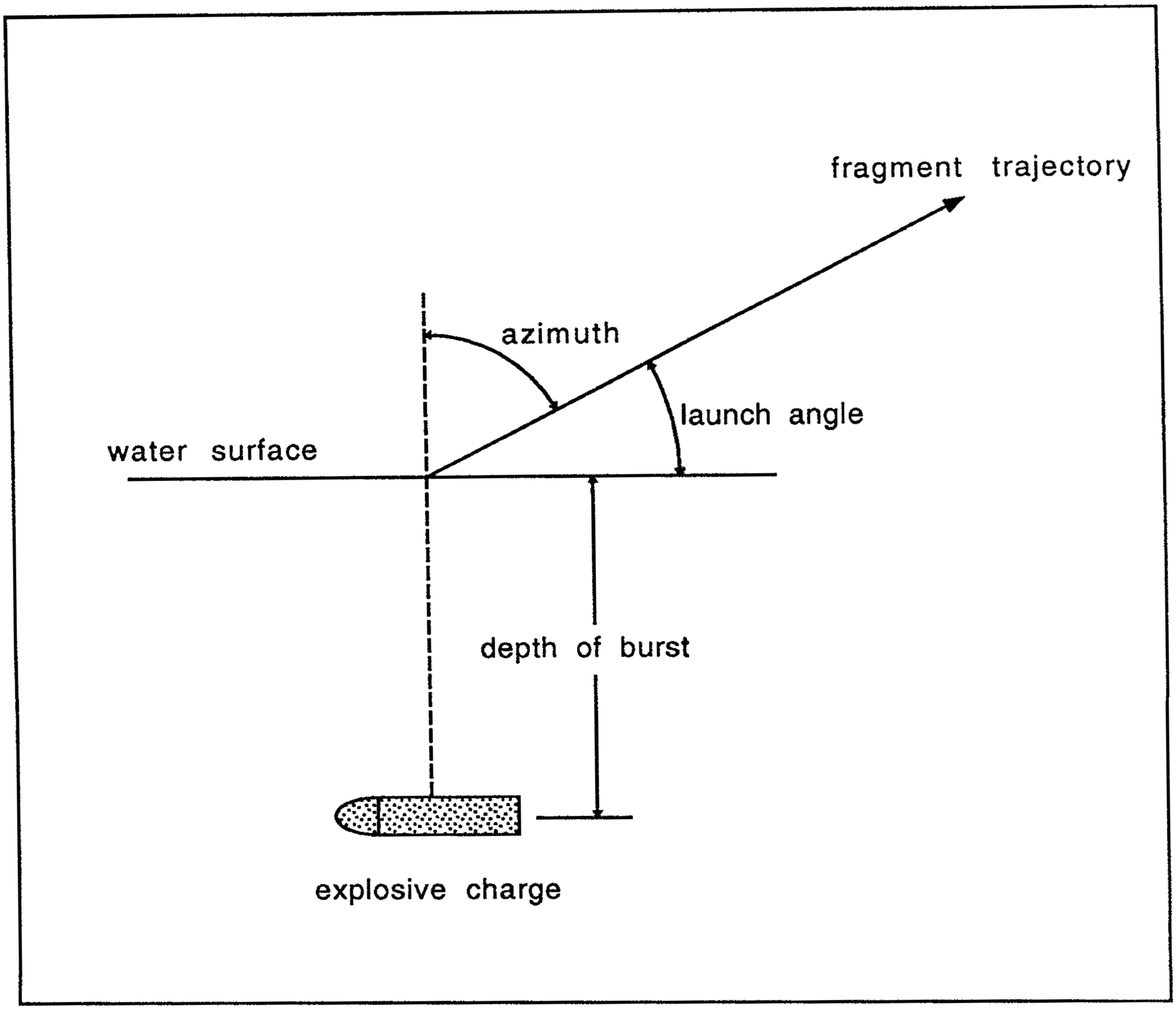

FIGURE 6. FRAGMENTATION FROM UNDERWATER EXPLOSIONS

FIGURE 7. FRAGMENT VELOCITY VERSUS SCALED DEPTH OF BURST

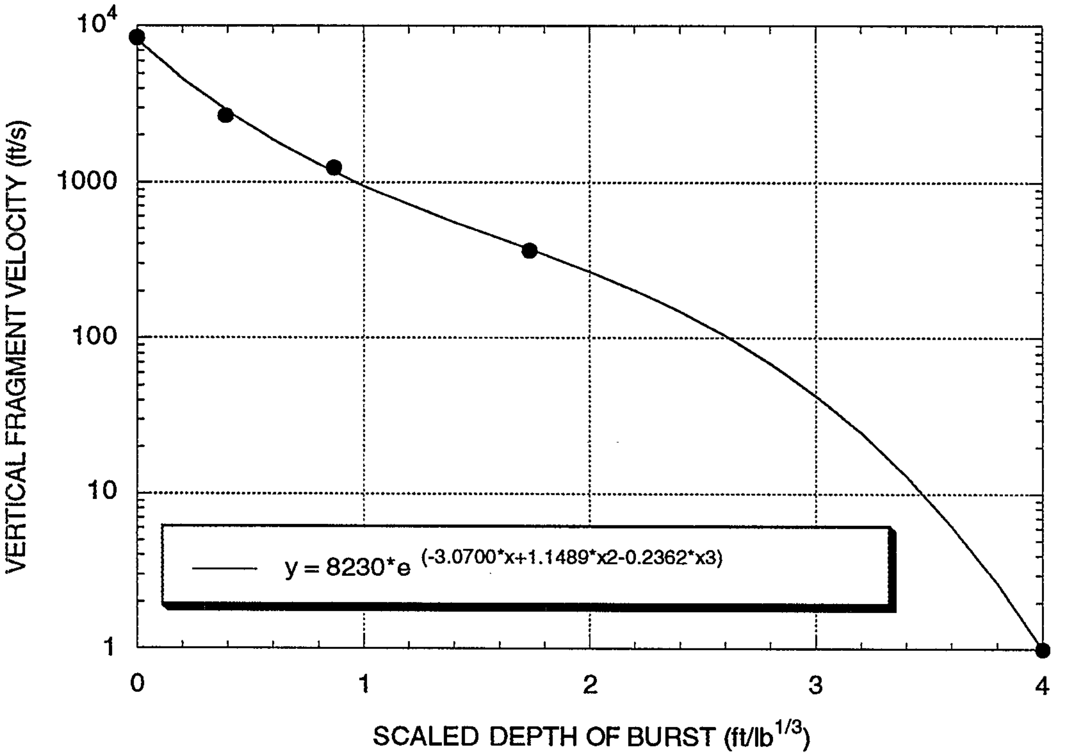

FIGURE 8. FRAGMENT VELOCITY VERSUS AZIMUTH

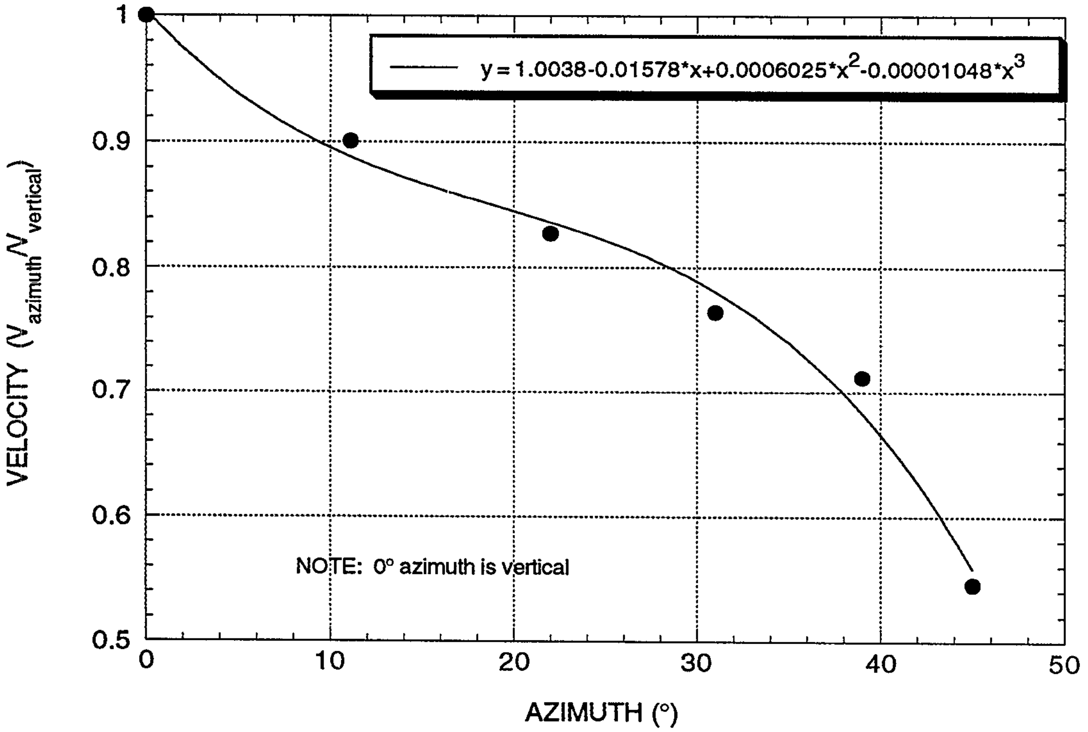

FIGURE 9. MAXIMUM AZIMUTH ANGLE VERSUS SCALED DEPTH OF BURST

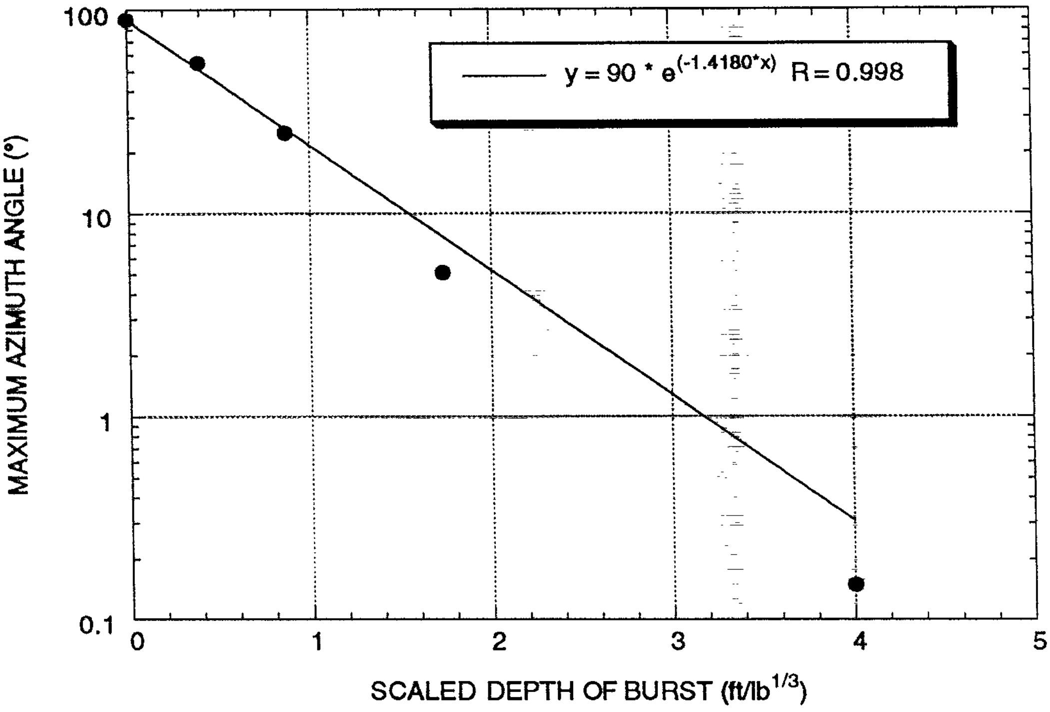

TABLE 1. CURVE FIT COEFFICIENTS

SCALED DEPTH OF BURST (ft/lb^1/3)	COEFFICIENT	SLOPE	GOODNESS OF FIT
0.306	265.660	-1.531	0.961
0.509	119.370	-1.374	0.989
0.688	79.583	-1.246	0.974
0.740	30.647	-1.103	0.989
0.893	12.535	-1.020	0.997
1.110	12.149	-1.009	0.998
3.000	2.301	-0.931	0.898
3.713	1.717	-0.819	1*
5.570	3.846	-1.078	1*
6.498	1.657	-0.930	1*

*limited data

NOTE: For each depth, P=coefficient*scaled range ^ (slope)

TABLE 2. QUARRY AIRBLAST

Charge Weight (lb)	Booster Type	Booster Weight (lb)	Charge Depth (ft)	Maximum Pressure (psi)	Weight Factor	Eff. Charge Weight (lbs)	Scaled Depth (ft/lb^1/3)	Scaled Range (ft/lb^1/3)	Coefficient	Average Coefficient
27.28	Pentolite	2.901	50	0.00606	1.53	44.56	14.1	60.5	0.367	
27.11	Pentolite	2.865	50	0.00725	1.53	44.26	14.1	60.6	0.440	
26.36	Pentolite	2.822	50	0.00633	1.50	42.36	14.3	61.5	0.390	
26.09	Pentolite	2.831	50	0.00604	1.49	41.79	14.4	61.8	0.373	
25.80	Pentolite	2.820	50	0.00751	1.50	41.52	14.4	61.9	0.466	
25.58	Pentolite	2.854	50	0.00747	1.50	40.34	14.6	62.5	0.468	
24.93	Pentolite	2.803	50	0.00763	1.54	40.34	14.6	62.5	0.477	0.457
24.78	Pentolite	2.810	50	0.00682	1.54	40.11	14.6	62.7	0.428	
53.91	Pentolite	7.853	75	0.01120	1.70	96.85	16.3	46.7	0.523	0.525
53.36	Pentolite	7.327	75	0.01123	1.70	95.55	16.4	46.9	0.527	
48.95	Pentolite	7.200	75	0.00943	1.65	85.67	17.0	48.7	0.459	
48.07	Pentolite	7.455	75	0.01024	1.65	84.39	17.1	48.9	0.501	0.473
52.37	Pentolite	7.583	75	0.00935	1.50	83.79	17.1	49.0	0.458	
39.36	Pentolite	7.534	75	0.00944	1.66	70.62	18.1	51.9	0.490	
39.03	Pentolite	7.490	75	0.00949	1.66	70.04	18.2	52.0	0.494	0.478
38.15	Pentolite	7.563	75	0.00829	1.48	61.67	19.0	54.3	0.450	
37.15	Pentolite	7.519	75	0.00875	1.48	60.16	19.1	54.7	0.479	
23.80	None		50	0.00489	0.69	16.42	19.7	84.4	0.412	0.389
10.64	Pentolite	0.154	50	0.00429	1.50	16.07	19.8	85.0	0.365	
8.03	Pentolite	0.153	50	0.00336	1.50	12.15	21.7	93.3	0.314	0.318
7.05	Pentolite	0.155	50	0.00287	1.50	10.68	22.7	97.4	0.280	
7.00	Pentolite	0.154	50	0.00285	1.50	10.61	22.8	97.6	0.278	
45.00	None		75	0.00586	0.69	31.05	23.9	68.2	0.400	

NOTE: COEFFICIENT = MAXIMUM PRESSURE * SCALED RANGE

TABLE 3. CURVE FIT COEFFICIENTS--DATA BASE

SCALED DEPTH OF BURST (ft/lb^1/3)	COEFFICIENT	SLOPE	GOODNESS OF FIT
0.306	265.660	-1.531	0.961
0.509	119.370	-1.374	0.989
0.688	79.583	-1.246	0.974
0.740	30.647	-1.103	0.989
0.893	12.535	-1.020	0.997
1.110	12.149	-1.009	0.998
3.000	2.301	-0.931	0.898
3.713	1.717	-0.819	1*
5.570	3.846	-1.078	1*
6.498	1.657	-0.930	1*
14.400	0.457	assumed to be -1	
16.400	0.525	assumed to be -1	
17.100	0.437	assumed to be -1	
18.600	0.478	assumed to be -1	
19.700	0.389	assumed to be -1	
22.800	0.318	assumed to be -1	

*limited data

NOTE: For each depth, P=coefficient*scaled range ^ (slope)

TABLE 4. WEIGHT AND VELOCITY FACTORS

EXPLOSIVE	WEIGHT FACTOR	VELOCITY FACTOR
TNT	0.69	0.87
PENTOLITE	0.69	0.98
HBX-1	1.00	0.94
HBX-3	1.30	0.84
H-6	1.14	1.00
PBXN-103	1.52	1.00
COMPOSITION C4	0.71	1.02
Other Plastic Bonded Underwater Explosives	1.5-1.72	0.8-1.2

TABLE 5. AIRBLAST CURVE FIT CONSTANTS FOR VARYING SCALED DEPTHS OF BURST

SCALED DEPTH	SLOPE	COEFFICIENT		SCALED DEPTH	SLOPE	COEFFICIENT
0.30	-1.56	248.17		3.00	-1.00	3.39
0.35	-1.52	216.78		3.20	-1.00	3.15
0.40	-1.48	187.59		3.40	-1.00	2.94
0.45	-1.43	160.60		3.60	-1.00	2.76
0.50	-1.39	135.81		3.80	-1.00	2.60
0.55	-1.34	113.22		4.00	-1.00	2.45
0.60	-1.29	92.83		4.20	-1.00	2.32
0.65	-1.24	74.65		4.40	-1.00	2.20
0.70	-1.19	58.67		4.60	-1.00	2.10
0.75	-1.14	44.89		4.80	-1.00	2.00
0.80	-1.10	33.31		5.00	-1.00	1.91
0.85	-1.06	23.93		5.50	-1.00	1.71
0.90	-1.04	16.76		6.00	-1.00	1.56
0.95	-1.02	12.32		6.50	-1.00	1.42
1.00	-1.01	11.63		7.00	-1.00	1.31
1.10	-0.99	10.45		7.50	-1.00	1.21
1.20	-0.99	9.48		8.00	-1.00	1.13
1.30	-0.99	8.66		8.50	-1.00	1.05
1.40	-0.99	7.97		9.00	-1.00	0.99
1.50	-0.99	7.38		9.50	-1.00	0.93
1.60	-0.99	6.86		10.00	-1.00	0.88
1.70	-0.99	6.41		11.00	-1.00	0.79
1.80	-1.00	6.01		12.00	-1.00	0.71
1.90	-1.00	5.66		13.00	-1.00	0.65
2.00	-1.00	5.34		14.00	-1.00	0.60
2.10	-1.00	5.06		15.00	-1.00	0.56
2.20	-1.00	4.80		16.00	-1.00	0.52
2.30	-1.00	4.56		17.00	-1.00	0.48
2.40	-1.00	4.35		18.00	-1.00	0.45
2.50	-1.00	4.16		19.00	-1.00	0.43
2.60	-1.00	3.98		20.00	-1.00	0.40
2.70	-1.00	3.81				
2.80	-1.00	3.66				
2.90	-1.00	3.52				

P=coefficient*scaled range^(slope)

TABLE 6. EXAMPLE 1--FRAGMENT RANGE

DEPTH (ft)	CHARGE WEIGHT (lbs)	SCALED DEPTH (ft/lb^1/3)	MAXIMUM AZIMUTH (°)	VERTICAL VELOCITY (ft/s)
2.25	192	0.39	52	2919
VELOCITY FACTOR = 1.0				
AZIMUTH (°)	**AZIMUTH FACTOR**	**VELOCITY (ft/s)**	**LAUNCH ANGLE (°)**	**RANGE (ft)**
0	1.00	2919	90	
5	0.94	2740	85	314
10	0.90	2615	80	621
15	0.87	2531	75	903
20	0.85	2467	70	1181
25	0.82	2400	65	1432
30	0.79	2305	60	1652
35	0.74	2161	55	1826
40	0.67	1944	50	1932
45	0.56	1631	45	1956
46	0.53	1555	44	1947
47	0.50	1474	43	1933
48	0.48	1388	42	1913
49	0.44	1297	41	1886
50	0.41	1200	40	1894
51	0.38	1097	39	1899
52	0.34	989	38	1897

TABLE 7. EXAMPLE 2--FRAGMENT RANGE

DEPTH (ft)	CHARGE WEIGHT (lbs)	SCALED DEPTH (ft/lb^1/3)	MAXIMUM AZIMUTH (°)	VERTICAL VELOCITY (ft/s)
16	10000	0.74	31	1354
VELOCITY FACTOR = 0.94				
AZIMUTH (°)	**AZIMUTH FACTOR**	**VELOCITY (ft/s)**	**LAUNCH ANGLE (°)**	**RANGE (ft)**
0	1.00	1354	90	
5	0.94	1271	85	528
10	0.90	1213	80	1058
15	0.87	1174	75	1541
20	0.85	1144	70	2018
25	0.82	1113	65	2451
26	0.82	1105	64	2528
27	0.81	1097	63	2603
28	0.80	1089	62	2677
29	0.80	1079	61	2749
30	0.79	1069	60	2818
31	0.78	1058	59	2888